Irreversible Mesoscale Fluctuations Herald the Emergence of Dynamical Phases

Thomas Suchanek,[1] Klaus Kroy,[1] and Sarah A. M. Loos[2,*]

[1]*Institut für Theoretische Physik, Universität Leipzig, Postfach 100 920, D-04009 Leipzig, Germany*
[2]*DAMTP, Centre for Mathematical Sciences, University of Cambridge, Wilberforce Road, Cambridge CB3 0WA, United Kingdom*

We study fluctuating field models with spontaneously emerging dynamical phases. We consider two typical transition scenarios associated with parity-time symmetry breaking: oscillatory instabilities and critical exceptional points. An analytical investigation of the low-noise regime reveals a drastic increase of the mesoscopic entropy production toward the transitions. For an illustrative model of two nonreciprocally coupled Cahn-Hilliard fields, we find physical interpretations in terms of actively propelled interfaces and a coupling of eigenmodes of the linearized dynamics near the critical exceptional point.

When Einstein's paper on Brownian motion appeared, he received a critical letter from Röntgen [1] who reiterated the historically widespread concern that such "motion from heat" would violate the second law. He failed to understand that Einstein had just made precise the centuries-old notion of heat being but a name for the incessant random motion of the molecular constituents of all macroscopic matter [2]. In fact, these thermal fluctuations are a manifestation of conservation, not production, of energy and entropy, according to the fluctuation-dissipation theorem [3]. However, this cornerstone of modern equilibrium statistical mechanics is lost far from equilibrium, where it becomes a central task to understand whether, when, and why mesoscopic fluctuations produce entropy. With regard to biological systems, this literally becomes a question of "life and death."

A fundamental property of any thermal equilibrium is time-reversal symmetry. Its breaking, in turn, is associated with a production of entropy and dissipative dynamics. Notably, on the coarse-grained scale, however, only part of the full entropy production is generally perceptible. A versatile measure to quantify time-reversal symmetry breaking (TRSB) is then the log-ratio of probabilities for forward and backward paths of the coarse-grained dynamics [4–7]. This so-called (informatic) entropy production rate $\mathcal{S}$ and related measures have recently been studied for a variety of systems; from single or few particle models [6], over nonequilibrium field theories of active matter [8–12], to experimental studies on multiscale biological systems [13–15].

In this Letter, we explore how TRSB of mesocale fluctuations in many-body systems informs us about incipient pattern formation. Specifically, we address the TRSB associated with the emergence of *dynamical* mesophases, such as persistent traveling or oscillating patterns [16–28]. Such states are paradigmatic examples of dissipative structures maintained by permanent dissipative energy currents [29–32]. Their spontaneous emergence is an instructive example of how a hidden nonequilibrium condition and its entropy production may reveal themselves mesoscopically. For example, for the so-called Brusselator model, it was recently shown that $\mathcal{S}$ may display a significant increase across the static-dynamic phase transitions to its oscillating phase [10].

In the following, we consider a broad class of nonequilibrium field models with conserved dynamics, and focus on two most common static-dynamic transition scenarios: oscillatory instabilities [30,33], which are field-theoretical manifestations of a Hopf bifurcation, and critical exceptional points (CEP) [34,35], which arise by coalescence of a Goldstone and a critical mode. Both these very dissimilar scenarios can be addressed within the framework of non-Hermitian field theories [36]. As was described only recently, CEPs generically occur in many-body systems with nonreciprocal interactions [35,37–41], i.e., interactions that violate the action-reaction principle [42]. For both scenarios, we show that the approach from the static toward the dynamic phase is accompanied by a surge in entropy production that scales like the susceptibility. Further, we discover general connections between the parity-time ($\mathcal{PT}$) symmetry breaking that generically occurs at CEPs [35,43,44], on the one hand, and the emergence of irreversible, i.e., TRSB fluctuations, on the other hand. Here, and more comprehensively in a companion article [45], we illustrate our general findings with a model of two nonreciprocally coupled Cahn-Hilliard field equations [37–40].

Field theory and symmetry breaking.—We study hydrodynamic models of the following structure:

$$\dot{\phi}_i = -\nabla \cdot \boldsymbol{J}_i, \qquad \boldsymbol{J}_i = -\nabla \mu_i + \sqrt{2\epsilon}\boldsymbol{\Lambda}_i, \qquad (1)$$

with N scalar field components $\phi_i(\boldsymbol{r}, t)$, $i = 1, \dots, N$, representing conserved order parameters, such as the species number densities, of an active many-body system and their currents $\boldsymbol{J}_i(\boldsymbol{r}, t)$ [41,46]. The Gaussian space-time white noise term $\sqrt{2\epsilon}\boldsymbol{\Lambda}_i(\boldsymbol{r}, t)$ is constructed such that, in the equilibrium case, where $\mu_i[\phi]$ derives from a free energy functional $\mathcal{F}[\phi]$, i.e., $\mu_i = \delta\mathcal{F}/\delta\phi_i$, the resulting statistical field theory would obey a fluctuation-dissipation relation [3], with ϵ denoting the noise intensity. However, for the case of a nonequilibrium deterministic current $\boldsymbol{J}_i^{\mathrm{d}}[\phi] \equiv -\nabla\mu_i[\phi]$, which is of interest here, the chemical potential μ_i cannot be represented as a gradient. To exclude externally driven systems, we further assume that Eq. (1) is invariant with respect to parity inversion, $\mathcal{P}: \boldsymbol{r} \mapsto -\boldsymbol{r}$.

A first useful insight is that, by construction, the spontaneous emergence of phases with traveling patterns in models of the type of Eq. (1) is always accompanied by a breaking of $\mathcal{PT}$ symmetry. This can be seen as follows. In a phase with traveling patterns, the zero-noise limit ($\epsilon \to 0$) of Eq. (1) has solutions of the form $\phi_i^*(\boldsymbol{r}, t) \equiv \varphi_i(\boldsymbol{r} - \boldsymbol{v}t)$. Then, the $\mathcal{P}$ invariance of Eq. (1) implies that $\varphi_i'(\boldsymbol{r} + \boldsymbol{v}t)$, with $\varphi_i'(\boldsymbol{x}) = \mathcal{P}\varphi_i(\boldsymbol{x}) = \varphi_i(-\boldsymbol{x})$ is also a solution; which can as well be expressed as $\varphi_i'(\boldsymbol{r} + \boldsymbol{v}t) = \mathcal{T}\varphi_i'(\boldsymbol{r} - \boldsymbol{v}t)$, with $\mathcal{T}$ the time-inversion operator. Therefore, the $\mathcal{PT}$ operation applied to any given traveling pattern solution of Eq. (1) yields another solution. Now, it is clear that, on the one hand, a parity symmetric pattern (i.e., $\varphi' = \varphi$) can occur only for $\boldsymbol{v} = 0$, and that, on the other hand, spontaneously emerging dynamical solutions φ with $\boldsymbol{v} \neq 0$ automatically cease to be $\mathcal{PT}$ eigenfunctions. Note that the emergence of $\mathcal{PT}$-broken dynamical phases is not specific to field models of the type of Eq. (1) but observed in a much wider context, comprising polar swarm models [11,35], directional solidification [47], or driven interfaces [48,49].

Irreversibility.—To study irreversibility, we employ a framework [8,9] that defines the entropy production $s[\phi; 0, T]$ along a trajectory $\{\phi_{t \in [0,T]}\}$ as the log ratio of forward and backward path probabilities (see Ref. [36] for details). The average rate of entropy production, $\mathcal{S} = \lim_{h \to 0} \langle s[\phi; t, t+h]/h \rangle$, serves as a measure of the breaking of detailed balance and of time-reversal symmetry, at time t, where $\langle . \rangle$ denotes the noise average. A main result of Ref. [9] was that it can, in the steady state, be expressed as the volume integral $\mathcal{S} = -\epsilon^{-1} \sum_i \int_V d\boldsymbol{r} \langle \dot{\phi}_i \mu_i \rangle$, which is understood to be UV regularized. By employing the Itô calculus of functionals [50], we derive, as a central result of the companion paper [36], the more explicit form

$$\mathcal{S} = \int_V d\boldsymbol{r} \frac{\sum_i \langle |\boldsymbol{J}_i^{\mathrm{d}}|^2 \rangle}{\epsilon} + \int_V d\boldsymbol{r} \sum_i \left\langle \frac{\delta}{\delta\phi_i} \nabla \cdot \boldsymbol{J}_i^{\mathrm{d}} \right\rangle. \quad (2)$$

It yields $\mathcal{S}$ based on the single time probability distribution of ϕ alone, which is particularly useful to study phase transitions.

We now consider the linear stability of the zero-noise solutions ϕ^* of our dynamical system, i.e., the eigensystem of the Jacobian $(\mathcal{J}_{\phi*})_{ij} = -\delta(\nabla \cdot \boldsymbol{J}_i^{\mathrm{d}})/\delta\phi_j^*$, represented in a Fourier basis. A mode (eigenvector) becomes unstable when the real part of its eigenvalues vanishes. Because of the parity symmetry of Eq. (1), $\mathcal{J}_{\phi*}$ is real. Crucially, we allow $\mathcal{J}_{\phi*}$ to be *non-Hermitian*, thereby capturing a wide variety of nonequilibrium conditions [35,51]. A common route from a (mesoscopically) static state to a dynamical state is via oscillatory instabilities. They occur through a pair of complex conjugated eigenmodes of $\mathcal{J}_{\phi*}$ that become unstable and whose eigenvalues (here denoted by $\lambda_\pm$) have nonvanishing imaginary parts. In contrast, the alternative scenario of a CEP is not primarily characterized by the properties of the eigenvalues of $\mathcal{J}_{\phi*}$, but by the fact that the modes that loose stability in the course of the transition *align*. In the following, we assume that a transition involving only two modes $\hat{e}_0$, $\hat{e}_1$ with eigenvalues λ_0 and λ_1. If one of them is a Goldstone mode of a broken continuous symmetry (such as space translation invariance or $O(N)$ symmetry [52]) so that $\lambda_0 = 0$ for $\hat{e}_0$, the CEP leads into a dynamical phase, which dynamically restores the continuous symmetry associated with this Goldstone mode [35,36].

Using Eq. (2), we deduce general characteristics of the entropy production rate $\mathcal{S}$ in the vicinity of the transitions. Thereby, the limit $\mathcal{S}^* \equiv \lim_{\epsilon \to 0} \mathcal{S}$ is particularly informative, revealing the leading order contribution to TRSB in ϵ which dominates the entire low noise regime and has universal (model-independent) character. Our first general finding is that in static phases with non-Hermitian dynamics, $\mathcal{S}^*$ is generally of order ϵ^0, i.e., they exhibit TRSB even for arbitrarily low noise intensity. Near oscillatory instabilities of monochromatic modes of wavelength $2\pi/|\boldsymbol{q}^k|$, $\mathcal{S}^*$ behaves like

$$\mathcal{S}^* \sim |\boldsymbol{q}^k|^{-2} |\mathrm{Im}\lambda_\pm|^2 \chi, \quad \text{as } \mathrm{Re}\lambda_\pm \to 0, \quad (3)$$

where $\chi \equiv \lim_{\epsilon \to 0} \epsilon^{-1} \sum_i \int_V d\boldsymbol{r} \langle |\phi_i - \phi_i^*|^2 \rangle$ is the system's static susceptibility, which scales like $|\mathrm{Re}\lambda_\pm|^{-1}$, close to the transition. The proof and the general expression is presented in Ref. [36]. Similarly, for the CEP, we find

$$\mathcal{S}^* \propto \chi \propto \lambda_1^{-1}, \quad \text{as } \lambda_1 \to 0. \quad (4)$$

Here, the most notable insight is that, in any case, we can identify a component $\boldsymbol{J}_0^{\mathrm{d}} \equiv \hat{P}_0 \boldsymbol{J}^{\mathrm{d}}$, of the deterministic current along $\hat{e}_0$ as the primary source of irreversibility [53], so that $\mathcal{S}^*$ is dominated by $\int_V d\boldsymbol{r} \langle |\boldsymbol{J}_0^{\mathrm{d}}|^2 \rangle / \epsilon$. This current is generated by a one-way coupling from damped modes to the Goldstone mode, which entails a giant noise

amplification in the latter [36]. From Eqs. (3), (4), we conclude that, for both types of transitions, $\mathcal{S}$ is determined by the inverse of the real part of the eigenvalue that becomes unstable across the transition. Thus, the static phases exhibit, close to the transitions, massively growing (and for $\epsilon \to 0$ diverging) irreversibility, despite their lack of systematic transport, and despite their seemingly equilibriumlike character. In contrast, across conventional critical points (and generally transitions that are accompanied by the sign change of a single real eigenvalue), $\mathcal{S}$ remains regular, despite diverging χ [36].

Within the dynamical phase itself, the small-noise expansion [54] of Eq. (2) with respect to ϕ^* yields [36]

$$\mathcal{S} = \epsilon^{-1} \sum_i \int_V d\boldsymbol{r} |\boldsymbol{J}_i^d(\phi^*)|^2 + \mathcal{O}(\epsilon^0). \tag{5}$$

Since the deterministic current is not sensitive to ϵ, $\mathcal{S} \sim \epsilon^{-1}$ to leading order. If the dynamical phase admits a traveling pattern $\phi_i^*(\boldsymbol{r}, t) \equiv \varphi_i(\boldsymbol{r} - \boldsymbol{v}t)$, Eq. (5) takes the more explicit form $\mathcal{S} = \epsilon^{-1}|\boldsymbol{v}|^2 \sum_i \int_V d\boldsymbol{r} |\varphi_i|^2 + \mathcal{O}(\epsilon^0)$, revealing that $\mathcal{S}$ originates from the hydrodynamic mesoscopic mass fluxes $\boldsymbol{v}|\varphi_i|$.

Illustrative example.—To illustrate our general findings, we consider a concrete model of the type of Eq. (1), namely, a stochastic version of the nonreciprocal Cahn-Hilliard model [37–40]. It is simple enough to be analytically traceable, while still exhibiting a dynamical phase, which is accesible via a CEP and an oscillatory instability. The dynamical equations for the two-component field $\phi = (\phi_A, \phi_B)^T$ read

$$\dot{\phi}_A = \nabla[(\alpha + \phi_A^2 - \gamma\nabla^2)\nabla\phi_A + (\kappa - \delta)\nabla\phi_B + \sqrt{2\epsilon}\Lambda_A],$$
$$\dot{\phi}_B = \nabla[\beta\nabla\phi_B + (\kappa + \delta)\nabla\phi_A + \sqrt{2\epsilon}\Lambda_B]. \tag{6}$$

The nonreciprocal coupling δ between ϕ_A and ϕ_B ensures that the equations cannot be derived from a scalar potential and represent a non-Hermitian, nonequilibrium model. We study the dynamics on the one-dimensional domain $[0, 2\pi]$ with periodic boundary conditions, where the emergence of a dynamical phase itself, and the general features of the phase diagram, do not depend on the system size. The noise-free ($\epsilon = 0$) case of Eq. (6) was shown to exhibit three distinct phases [37]: a homogeneous phase ($\phi_{A,B}^* = 0$) for small negative α and two inhomogeneous "demixed" phases for large negative α. The approximate solution in terms of the dominant first Fourier mode $\phi_{A,B}^{1,*}(r, t) = \mathcal{A}_{A,B}^{1,*} \cos[r + \theta_{A,B}^{1,*}(t)]$ amounts to a static demixed phase for $\delta < \delta_c = \sqrt{\beta^2 + \kappa^2}$, when $\dot{\theta}_{A,B}^{1,*}(t) = 0$, and to a traveling-wave phase for $\delta > \delta_c$, when $\dot{\theta}_{A,B}^{1,*}(t) = \boldsymbol{v} = \pm\sqrt{\delta^2 - \delta_c^2}$, with both signs of the propagation velocity $\boldsymbol{v}$ being equally likely. The transition from the homogeneous to the traveling-wave state is through an

oscillatory instability, while the (secondary) phase transition from the static-demixed state to the traveling-wave state is via a CEP. We simulated Eq. (6) using a Euler-Maruyama algorithm with finite difference gradients, where the domain was discretized by equally spaced mesh points. For more details about the analytical and numerical treatment, we refer to our companion article [45]. Beyond the general Eqs. (3)–(5), it confirms that the entropy production scales like $\sim\epsilon^0$ in the static (homogeneous and demixed) phases, with singularities of $\mathcal{S}^*$ at the transitions to the traveling-wave phase, and diverging $\mathcal{S}^*$ in the traveling-wave state itself.

In the remainder, we exploit the explicit model, Eq. (6), to provide a physical interpretation of our general findings. In particular, we reveal which physical mechanism gives rise to the entropy production (and ultimately its divergence), as the transition is approached.

Let us first consider the dynamical phase itself. The sublinear scaling of $\mathcal{S}$ in ϵ, Eq. (5), indicates that the dynamical phase exhibits a macroscopic arrow of time. Recalling its definition in terms of path probabilities, a divergent $\mathcal{S}^*$ means that, upon observation of an (arbitrarily short) realization of the dynamics, one can be 100% sure in which direction time evolves. Where does this certainty come from? The sign of $\boldsymbol{v}$ is spontaneously determined by the initial condition and noise, only. Thus, the mere propagation of the wave alone *cannot* introduce an arrow of time. However, closer inspection of the solutions of Eq. (6) shows that the propagation velocity $\boldsymbol{v}$ is aligned with a characteristic phase shift $\langle\Delta\theta^\pi\rangle \neq 0$, with $\Delta\theta^\pi \equiv \theta_A^1 - (\theta_B^1 + \pi)$. The maxima of ϕ_B always "lag behind" the maxima of ϕ_A, as shown in Fig. 1(b). The alignment of $\boldsymbol{v}$ with $\langle\Delta\theta^\pi\rangle$ manifestly breaks $\mathcal{PT}$ symmetry and introduces the macroscopic arrow of time.
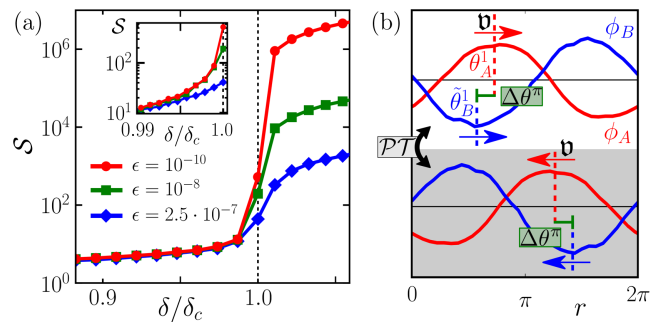

FIG. 1. Transition to a dynamical phase via a CEP. (a) Entropy production rate near the transition point δ_c from a static demixed to a traveling-wave phase in model Eq. (6) ($\alpha = -0.07$, $\gamma = 0.015$, $\kappa = 0.01$, $\beta = 0.05$), see Ref. [45] for simulation details. The inset shows a magnification. (b) Traveling-wave solution of Eq. (6) and its image under a parity transformation $\mathcal{P}$ (which yields an independent solution). The characteristic phase shift $\Delta\theta^\pi$ is always aligned with the propagation velocity $\boldsymbol{v}$ (indicated by arrows).
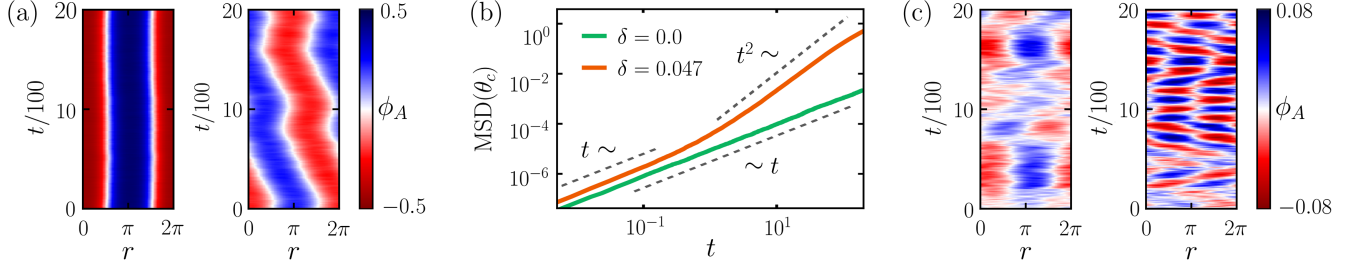
FIG. 2. Dynamics of the fluctuating Cahn-Hilliard model, Eq. (6), for $\epsilon = 2.5 \times 10^{-5}$ in the static phases: (a) Kymographs of the concentration field ϕ_A in the static-demixed phase ($\alpha = -0.07$), left: for the reciprocal equilibrium case ($\delta = 0$); right: close to the phase transition ($\delta = 0.92\delta_c = 0.047$). (b) The corresponding MSD of the center-of-mass variable θ_c. The ballistic regime ($\propto t^2$) signals persistent motion of the mean phase and the interfaces. (c) Kymographs of ϕ_A in the mixed phase, left: for the reciprocal case ($\delta = 0$, $\alpha = -0.013$); right: close to the oscillatory instability ($\delta = 0.06$, $\alpha = -0.063$).

Next, we turn to the static phases of Eqs. (6) and the unbounded increase of $\mathcal{S}^*$ toward the static-dynamic transitions predicted by Eqs. (3) and (4). A careful decomposition of the phase and amplitude fluctuations of $\phi_{A/B}$ in the static-demixed phase yields an interesting observation: close to the CEP, the fluctuating collective motion of the interfaces between the demixing profiles, represented by $\theta^1_{A,B}(t)$, produces most of the entropy [45]. As we show here, this entropy-generating interface motion is congruent to the irreversible motion of an "active particle" or microswimmer and results from systematic activations of the Goldstone mode. Formally, this can be seen as follows. Within the low noise regime, $\theta^1_{A,B}(t)$ can approximately be separated from higher modes, resulting in the closed equations of motion [45]

$$\dot{\theta}^1(t) = \mathbb{A} \cdot \theta^1 + \sqrt{\epsilon/2\pi}\xi, \qquad (7)$$

with $\theta^1 = (\theta^1_A, \tilde{\theta}^1_B)^T$, $\tilde{\theta}^1_B = \theta^1_B + \pi$, and $\langle \xi_i(t), \xi_j(t')\rangle = (2/\mathcal{A}^*_i)^2 \delta_{i,j}\delta(t - t')$, $i, j \in \{A, B\}$, and

$$\mathbb{A} = -\begin{pmatrix} (\kappa^2 - \delta^2)/\beta & -(\kappa^2 - \delta^2)/\beta \\ -\beta & \beta \end{pmatrix}. \qquad (8)$$

One eigenvalue of the dynamical operator $\mathbb{A}$ is strictly zero, $\lambda_0 = 0$, reflecting the native continuous translational symmetry of the model in Eq. (6), which is spontaneously broken in the static-demixed phase (giving rise to a Goldstone mode). The other eigenvalue is $\lambda_1 = -(\delta_c^2 - \delta^2)/\beta$. Now, expressing the phase dynamics (7), (8) in the "center-of-mass" frame, by applying the coordinate transformation $\theta_c \equiv (\Gamma_A\theta^1_A + \Gamma_B\tilde{\theta}^1_B)/\bar{\Gamma}$, $\Delta\tilde{\theta}^\pi \equiv \sqrt{\Gamma_A\Gamma_B}\bar{\Gamma}^{-1}\Delta\theta^\pi$, with $\Gamma_{A,B} \equiv \int_0^{2\pi} dr|\phi^{1,*}_{A,B}(r)|^2$, $\bar{\Gamma} = \Gamma_A + \Gamma_B$, yields

$$\partial_t\begin{pmatrix} \theta_c \\ \Delta\tilde{\theta}^\pi \end{pmatrix} = \begin{pmatrix} 0 & 2\delta \\ 0 & \lambda_1 \end{pmatrix}\begin{pmatrix} \theta_c \\ \Delta\tilde{\theta}^\pi \end{pmatrix} + \sqrt{2\epsilon/\bar{\Gamma}}\tilde{\xi}, \qquad (9)$$

with $\langle\tilde{\xi}_\mu\tilde{\xi}_\nu\rangle = \delta_{\mu\nu}\delta(t - t')$. It reveals that, for $|\delta| > 0$, θ_c performs a persistent random walk "propelled" by the

fluctuating phase shift $\Delta\theta^\pi$, in striking analogy to an active particle, with propulsion velocity $\mathfrak{v}_a \equiv 2\delta\Delta\tilde{\theta}^\pi$ in the active Ornstein-Uhlenbeck model [55,56]. The persistence time $t_p = 1/|\lambda_1|$ and $\langle|\mathfrak{v}_a|^2\rangle = 4\delta^2\epsilon/(\bar{\Gamma}|\lambda_1|)$ are controlled by the inverse eigenvalue λ_1^{-1} of the dynamical operator $\mathbb{A}$, which vanishes at the transition. This means that the interface between ϕ_A and ϕ_B fluctuates like the path of a microswimmer, which is, by itself, indicative of TRSB [57]. Indeed, this is visually evident from the exact numerical kymographs in Fig. 2(b). To obtain a quantitative comparison with the interface dynamics of equilibrium demixing, we compute from Eq. (9) the mean squared displacement (MSD) of θ_c [58], and find

$$\text{MSD}(\theta_c) = \begin{cases} \frac{\epsilon}{\bar{\Gamma}}\left(t + \frac{\delta^2}{2\lambda_1}t^2\right), & t \ll t_p \\ \frac{\epsilon}{\bar{\Gamma}}\left(1 + \frac{\delta^2}{\lambda_1^2}\right)t, & t \gg t_p \end{cases}. \qquad (10)$$

Clearly, the "activity" for $|\delta| > 0$ is revealed by a ballistic intermediate regime and a strongly enhanced late-time diffusion coefficient in the vicinity of the transition ($\lambda_1 \to 0$). The predictions of our approximate solution are nicely confirmed by the numerical data presented in Fig. 2(a) showing the MSD of the interface dynamics obtained directly from Eq. (6). The "active fluctuations" of the interface dynamics in the static demixed phase represent a concrete manifestation of TRSB on timescales comparable to the persistence time—in the same manner as it does for an active swimmer (note that here both fields $\phi_{A,B}$ are even under time reversal [60]). As can immediately be gleaned from Eq. (9), this TRSB yields a considerable fraction $\mathcal{S}^*_{\theta_c} = \bar{\Gamma}\langle|\mathfrak{v}_a|^2\rangle \lesssim \mathcal{S}^*$ of the total entropy production. It is generated by the irreversible mesoscopic current $\propto \mathfrak{v}_a$, pointing along the Goldstone mode and originating from the dissipative coherent motion of both demixing profiles, represented by θ_c. As the transition to the dynamical phase is approached ($\delta \to \delta_c$), $\mathfrak{v}_a$ and t_p increase unboundedly, resulting in an unbounded increase of $\mathcal{S}^*$. Importantly, the persistent motion of θ_c in Eq. (9) is always

oriented *toward* the phase shift $\Delta\theta^\pi$ (which has zero mean, $\langle\Delta\theta^\pi\rangle = 0$, contrasting the permanently $\mathcal{PT}$ broken traveling-wave state), see Fig. 1(b). We emphasize that such one-way coupling between the damped modes (here $\Delta\theta^\pi$) and a Goldstone mode (here θ_c) that does not vanish at the transition is a hallmark of CEPs and only possible for non-Hermitian dynamical operators [36]. It can be understood as a maximum violation of detailed balance. In the vicintiy of the CEP, this generically leads to a diversion and amplification of fluctuations into the direction of the Goldstone mode, as was recently described in the context of quantum systems [34]. As we further elaborate for general field models of the type of Eq. (6) in Ref. [36], this very mechanism is deeply connected with the origin of $\mathcal{PT}$ symmetry breaking at the CEP.

Lastly, also for the divergence of $\mathcal{S}^*$ at the oscillatory instability, the nonreciprocal Cahn-Hilliard model provides a rather intuitive interpretation. Noting that $|\text{Im}\lambda_\pm|$ corresponds to the frequency of the limit cycle, we find that $\mathcal{S}$ signals the presence of cyclic currents in the homogeneous phase. Their amplitude is entirely due to transient fluctuations, but eventually becomes systematically positive as χ diverges at the transition. In our example, this mechanism creates temporarily stable traveling waves, which are plainly obvious in the graphical representation of our simulation data in Fig. 2(c).

Conclusions.—We have studied the irreversible fluctuations of coarse-grained hydrodynamic field models close to the onset of dynamical phases. Clearly, the dynamical phase itself is a particularly drastic manifestation of TRSB. But our results show that, even before entering it, the nonequilibrium character of the dynamics reveals itself through transient TRSB fluctuations around a seemingly equilibriumlike average behavior. This observation could be of interest for a nonequilibrium classification of living matter [15]. Focusing on two paradigmatic transition scenarios, we uncovered that the fluctuations near $\mathcal{PT}$-breaking phase transitions not only inflate, as is in equilibrium critical phenomena, but also develop an asymptotically increasing time-reversal asymmetry and associated surging entropy production. In the low noise regime, $\mathcal{S}$ scales precisely as the susceptibility, or equivalently, as the inverse of the eigenvalue of the mode that becomes unstable across the transition. Moreover, we have drawn general connections between the $\mathcal{PT}$-symmetry breaking and TRSB of the fluctuations, at a CEP. We were able to attribute the striking simultaneous presence of two completely different forms of symmetry breaking ($\mathcal{PT}$ and TRSB) to a common origin, an active amplification of thermal noise into irreversible fluctuations. Our analysis of a model consisting of two nonreciprocally coupled noisy Cahn-Hilliard fields illustrates our general findings and provides instructive physical interpretations for the TRSB in terms of a peculiar phenomenology of "active interface dynamics." In future studies, it would be interesting to reconsider our findings from the perspective of "information thermodynamics," as recently pioneered for Turing patterns [61], and from the perspective of the renormalization group, as in Refs. [62–64]. Further, it would be worthwhile to investigate the spontaneously emerging mass current in the context of thermodynamics uncertainty relations [65–67].

Independent, consistent results for TRSB in the nonreciprocal Cahn-Hilliard model were reported in Ref. [68].

[*] sl2127@cam.ac.uk

[1] A. Einstein and M. Klein, *The Collected Papers of Albert Einstein: The Swiss Years: Correspondence, 1902–1914* (Princeton University Press, Princeton, NJ, 1993), p. 44.

[2] R. Hooke, *The Posthumous Works of Robert Hooke* (Routledge, Oxon and New York, 2019), p. 116.

[3] R. Kubo, The fluctuation-dissipation theorem, Rep. Prog. Phys. **29**, 255 (1966).

[4] J. L. Lebowitz and H. Spohn, A Gallavotti–Cohen-type symmetry in the large deviation functional for stochastic dynamics, J. Stat. Phys. **95**, 333 (1999).

[5] C. Maes and K. Netočný, Time-reversal and entropy, J. Stat. Phys. **110**, 269 (2003).

[6] U. Seifert, Entropy production along a stochastic trajectory and an integral fluctuation theorem, Phys. Rev. Lett. **95**, 040602 (2005).

[7] É. Roldán and J. M. R. Parrondo, Entropy production and Kullback-Leibler divergence between stationary trajectories of discrete systems, Phys. Rev. E **85**, 031129 (2012).

[8] Y. I. Li and M. E. Cates, Steady state entropy production rate for scalar Langevin field theories, J. Stat. Mech. (2021) 013211.

[9] C. Nardini, É. Fodor, E. Tjhung, F. van Wijland, J. Tailleur, and M. E. Cates, Entropy production in field theories without time-reversal symmetry: Quantifying the non-equilibrium character of active matter, Phys. Rev. X **7**, 021007 (2017).

[10] D. S. Seara, B. B. Machta, and M. P. Murrell, Irreversibility in dynamical phases and transitions, Nat. Commun. **12**, 392 (2021).

[11] Ø. Borthne, É. Fodor, and M. Cates, Time-reversal symmetry violations and entropy production in field theories of polar active matter, New J. Phys. **22**, 123012 (2020).

[12] G. Pruessner and R. Garcia-Millan, Field theories of active particle systems and their entropy production, arXiv:2211.11906.

[13] S. Ro, B. Guo, A. Shih, T. V. Phan, R. H. Austin, D. Levine, P. M. Chaikin, and S. Martiniani, Model-free measurement of local entropy production and extractable work in active matter, Phys. Rev. Lett. **129**, 220601 (2022).

[14] T. H. Tan, G. A. Watson, Y.-C. Chao, J. Li, T. R. Gingrich, J. M. Horowitz, and N. Fakhri, Scale-dependent irreversibility in living matter, arXiv:2107.05701.

[15] C. Battle, C. P. Broedersz, N. Fakhri, V. F. Geyer, J. Howard, C. F. Schmidt, and F. C. MacKintosh, Broken detailed balance at mesoscopic scales in active biological systems, Science **352**, 604 (2016).

[16] M. Bestehorn, R. Friedrich, and H. Haken, Traveling waves in nonequilibrium systems, Physica (Amsterdam) **37D**, 295 (1989).

[17] M. Bestehorn, R. Friedrich, and H. Haken, Two-dimensional traveling wave patterns in nonequilibrium systems, Z. Phys. B **75**, 265 (1989).

[18] S. Ghosh, S. Gutti, and D. Chaudhuri, Pattern formation, localized and running pulsation on active spherical membranes, Soft Matter **17**, 10614 (2021).

[19] S. Ramaswamy, J. Toner, and J. Prost, Nonequilibrium fluctuations, traveling waves, and instabilities in active membranes, Phys. Rev. Lett. **84**, 3494 (2000).

[20] M. Agrawal, I. R. Bruss, and S. C. Glotzer, Tunable emergent structures and traveling waves in mixtures of passive and contact-triggered-active particles, Soft Matter **13**, 6332 (2017).

[21] E. Frey, J. Halatek, S. Kretschmer, and P. Schwille, Protein pattern formation, in *Physics of Biological Membranes* (Springer, New York, 2018), pp. 229–260.

[22] K. C. Huang, Y. Meir, and N. S. Wingreen, Dynamic structures in Escherichia coli: Spontaneous formation of MinE rings and MinD polar zones, Proc. Natl. Acad. Sci. U.S.A. **100**, 12724 (2003).

[23] S.-i. Amari, Dynamic of pattern formation in lateral-inhibition type neural fields, Biol. Cybern. **27**, 77 (1977).

[24] J. Wang, Landscape and flux theory of non-equilibrium dynamical systems with application to biology, Adv. Phys. **64**, 1 (2015).

[25] S. Bhattacharya, T. Banerjee, Y. Miao, H. Zhan, P. Devreotes, and P. Iglesias, Traveling and standing waves mediate pattern formation in cellular protrusions, Sci. Adv. **6**, eaay7682 (2020).

[26] R. Welch and D. Kaiser, Cell behavior in traveling wave patterns of myxobacteria, Proc. Natl. Acad. Sci. U.S.A. **98**, 14907 (2002).

[27] S. Takada, N. Yoshinaga, N. Doi, and K. Fujiwara, Mode selection mechanism in traveling and standing waves revealed by min wave reconstituted in artificial cells, Sci. Adv. **8**, eabm8460 (2022).

[28] L. Demarchi, A. Goychuk, I. Maryshev, and E. Frey, Enzyme-enriched condensates show self-propulsion, positioning, and coexistence, Phys. Rev. Lett. **130**, 128401 (2023).

[29] A. Goldbeter, Dissipative structures in biological systems: Bistability, oscillations, spatial patterns and waves, Phil. Trans. R. Soc. A **376**, 20170376 (2018).

[30] M. C. Cross and P. C. Hohenberg, Pattern formation outside of equilibrium, Rev. Mod. Phys. **65**, 851 (1993).

[31] E. Tiezzi, R. Pulselli, N. Marchettini, and E. Tiezzi, *Dissipative Structures in Nature and Human Systems* (WIT press, Southhampton, 2008), pp. 293–299.

[32] B. N. Belintsev, Dissipative structures and the problem of biological pattern formation, Sov. Phys. Usp. **26**, 775 (1983).

[33] M. Cross and H. Greenside, Oscillatory patterns, in *Pattern Formation and Dynamics in Nonequilibrium Systems* (Cambridge University Press, Cambridge, England, 2009), pp. 358–400.

[34] R. Hanai and P. B. Littlewood, Critical fluctuations at a many-body exceptional point, Phys. Rev. Res. **2**, 033018 (2020).

[35] M. Fruchart, R. Hanai, P. B. Littlewood, and V. Vitelli, Non-reciprocal phase transitions, Nature (London) **592**, 363 (2021).

[36] T. Suchanek, K. Kroy, and S. A. M. Loos, companion article, Time-reversal and parity-time symmetry breaking in non-Hermitian field theories, Phys. Rev. E **108**, 064123 (2023).

[37] Z. You, A. Baskaran, and M. C. Marchetti, Nonreciprocity as a generic route to traveling states, Proc. Natl. Acad. Sci. U.S.A. **117**, 19767 (2020).

[38] S. Saha, J. Agudo-Canalejo, and R. Golestanian, Scalar active mixtures: The nonreciprocal Cahn-Hilliard model, Phys. Rev. X **10**, 041009 (2020).

[39] T. Frohoff-Hülsmann, J. Wrembel, and U. Thiele, Suppression of coarsening and emergence of oscillatory behavior in a Cahn-Hilliard model with nonvariational coupling, Phys. Rev. E **103**, 042602 (2021).

[40] T. Frohoff-Hülsmann and U. Thiele, Nonreciprocal Cahn-Hilliard equations emerging as one of eight universal amplitude equations, Phys. Rev. Lett. **131**, 107201 (2023).

[41] R. Mandal, S. S. Jaramillo, and P. Sollich, Robustness of travelling states in generic non-reciprocal mixtures, arXiv:2212.05618.

[42] S. A. M. Loos and S. H. L. Klapp, Irreversibility, heat and information flows induced by non-reciprocal interactions, New J. Phys. **22**, 123051 (2020).

[43] R. El-Ganainy, K. G. Makris, M. Khajavikhan, Z. H. Musslimani, S. Rotter, and D. N. Christodoulides, Non-Hermitian physics and PT symmetry, Nat. Phys. **14**, 11 (2018).

[44] A. Krasnok, N. Nefedkin, and A. Alu, Parity-time symmetry and exceptional points: A tutorial, arXiv:2103.08135.

[45] T. Suchanek, K. Kroy, and S. A. M. Loos, companion article, Entropy production in the nonreciprocal Cahn-Hilliard model, Phys. Rev. E **108**, 064610 (2023).

[46] M. Knežević, T. Welker, and H. Stark, Collective motion of active particles exhibiting non-reciprocal orientational interactions, Sci. Rep. **12**, 19437 (2022).

[47] P. Coullet, R. E. Goldstein, and G. H. Gunaratne, Parity-breaking transitions of modulated patterns in hydrodynamic systems, Phys. Rev. Lett. **63**, 1954 (1989).

[48] H. Z. Cummins, L. Fourtune, and M. Rabaud, Successive bifurcations in directional viscous fingering, Phys. Rev. E **47**, 1727 (1993).

[49] L. Pan and J. R. de Bruyn, Spatially uniform traveling cellular patterns at a driven interface, Phys. Rev. E **49**, 483 (1994).

[50] R. Cont and D. Fournie, A functional extension of the Ito formula, C. R. Math. **348**, 57 (2010).

[51] Y. Ashida, Z. Gong, and M. Ueda, Non-Hermitian physics, Adv. Phys. **69**, 249 (2020).

[52] C. P. Zelle, R. Daviet, A. Rosch, and S. Diehl, Universal phenomenology at critical exceptional points of nonequilibrium $o(n)$ models, arXiv:2304.09207.

[53] See Ref. [36] for the precise definition of the projector $\hat{P}_0$.

[54] C. Gardiner, *Stochastic Methods* (Springer, Berlin, 2009), Vol. 4.

[55] É. Fodor, C. Nardini, M. E. Cates, J. Tailleur, P. Visco, and F. van Wijland, How far from equilibrium is active matter?, Phys. Rev. Lett. **117**, 038103 (2016).

[56] L. Caprini, U. M. B. Marconi, A. Puglisi, and A. Vulpiani, The entropy production of Ornstein–Uhlenbeck active particles: A path integral method for correlations, J. Stat. Mech. (2019) 053203.

[57] G. Falasco, R. Pfaller, A. P. Bregulla, F. Cichos, and K. Kroy, Exact symmetries in the velocity fluctuations of a hot Brownian swimmer, Phys. Rev. E **94**, 030602(R) (2016).

[58] The MSD of θ_c is readily obtained by applying the results from Ref. [59] to Eq. (9). We further note that the MSD of the mean phase $\theta_{\mathrm{m}} \equiv (\theta_A^1 + \tilde{\theta}_B^1)/2$, which may be more accessible from an experimental perspective, exhibits the same ballistic short-time regime and the identical, enhanced long-time diffusion coefficient.

[59] G. Nguyen, R. Wittmann, and H. Löwen, Active Ornstein-Uhlenbeck model for self-propelled particles with inertia, J. Phys. Condens. Matter **34**, 035101 (2021).

[60] S. Shankar and M. C. Marchetti, Hidden entropy production and work fluctuations in an ideal active gas, Phys. Rev. E **98**, 020604(R) (2018).

[61] G. Falasco, R. Rao, and M. Esposito, Information thermodynamics of Turing patterns, Phys. Rev. Lett. **121**, 108301 (2018).

[62] M. Paoluzzi, Scaling of the entropy production rate in a φ^4 model of active matter, Phys. Rev. E **105**, 044139 (2022).

[63] F. Caballero and M. E. Cates, Stealth entropy production in active field theories near Ising critical points, Phys. Rev. Lett. **124**, 240604 (2020).

[64] A. Cavagna, L. Di Carlo, I. Giardina, T. S. Grigera, S. Melillo, L. Parisi, G. Pisegna, and M. Scandolo, Natural swarms in 3.99 dimensions, Nat. Phys. **19**, 1043 (2023).

[65] A. C. Barato and U. Seifert, Thermodynamic uncertainty relation for biomolecular processes, Phys. Rev. Lett. **114**, 158101 (2015).

[66] T. R. Gingrich, J. M. Horowitz, N. Perunov, and J. L. England, Dissipation bounds all steady-state current fluctuations, Phys. Rev. Lett. **116**, 120601 (2016).

[67] O. Niggemann and U. Seifert, Field-theoretic thermodynamic uncertainty relation: General formulation exemplified with the Kardar–Parisi–Zhang equation, J. Stat. Phys. **178**, 1142 (2020).

[68] H. Alston, L. Cocconi, and T. Bertrand, preceding Letter Irreversibility across a nonreciprocal $\mathcal{PT}$-symmetry-breaking phase transition, Phys. Rev. Lett. **131**, 258301 (2023).